

# Three-dimensional numerical investigations of the laser-beam interactions in an undulator<sup>\*</sup>

DENG Hai-Xiao(邓海啸)<sup>1;1)</sup> LIN Tang-Yu(林唐宇)<sup>2</sup> YAN Jun(颜俊)<sup>1</sup>  
WANG Dong(王东)<sup>1</sup> DAI Zhi-Min(戴志敏)<sup>1</sup>

<sup>1</sup> Shanghai Institute of Applied Physics, Chinese Academy of Sciences, Shanghai 201800, China

<sup>2</sup> Department of Physics, East China Normal University, Shanghai 200062, China

**Abstract:** Laser-beam interaction in an undulator is commonly suggested in the development of free electron laser (FEL) schemes. In this paper, a three-dimensional algorithm is developed to assist in laser-beam interaction simulation in an undulator, which is built on the basis of the fundamentals of electrodynamics, i.e. the electron's behavior is determined by the magnetic field and the laser electric field in the time domain. On the basis of the algorithm, the detuning effect in a laser heater, the carrier envelope phase effect of a few-cycle laser in attosecond X-ray FEL schemes and output wavelength tuning in a high gain harmonic generation FEL are numerically discussed.

**Key words:** detuning, laser-heater, few-cycle laser, carrier envelope phase

**PACS:** 41.60.Cr      **DOI:** 10.1088/1674-1137/35/3/018

## 1 Introduction

In recent years, people have become increasingly interested in the development of a high-gain short-wavelength free electron laser (FEL), which is a powerful light source capable of providing coherent radiation pulses in the spectral range from infrared to hard X-ray. Self-amplified spontaneous emission (SASE) FEL [1–3] and various seeded FELs [4–7] are two leading candidates currently pursued in the design of 4<sup>th</sup> generation light sources. SASE begins from the initial shot noise of the electron beam and results in a radiation with excellent spatial coherence, but rather poor temporal coherence. In contrast, seeded FEL allows us to produce radiation pulses with both spatial and temporal coherence.

In general, a seeded FEL consists of 3 components. At first, the electron beam's energy is modulated by a seed laser in a modulator undulator. Next, the energy modulation is converted into a spatial one when the electron beam passes through a dispersive chicane and thus abundant harmonics bunching is produced in the electron beam's density distribution. Finally, when the spatially modulated electron beam enters a

radiator undulator, which is designed to resonate to one of the harmonics of the seed laser, rapid coherent emission at this resonant harmonic is produced and amplified exponentially until saturation. As demonstrated in recent papers [8–10], several improvements to seeded FELs have been carried out by using the double-modulator structure and even two seed lasers.

Simultaneously, the suppression of the electron beam's microbunching instability [11–13] by using a laser-induced energy spread in an undulator has been experimentally demonstrated in a linac-coherent light source (LCLS) [14], which is the first hard X-ray FEL in the world. Moreover, interaction between the electron beam and the high intensity few-cycle laser in an undulator or a short wiggler is widely proposed in novel FEL schemes for femtosecond and attosecond pulse generation [15–20]. Obviously, more and more laser-beam interactions in undulators are being introduced into FELs to obtain various types of energy modulations.

Laser-beam interaction was conventionally studied in the FEL community using the undulator-period-averaged FEL equations [21–25], which was first shown by Kroll, Morton and Rosenbluth. How-

---

Received 22 June 2010

<sup>\*</sup> Supported by Shanghai Natural Science Foundation (09JC1416900)

1) E-mail: denghaixiao@sinap.ac.cn

©2011 Chinese Physical Society and the Institute of High Energy Physics of the Chinese Academy of Sciences and the Institute of Modern Physics of the Chinese Academy of Sciences and IOP Publishing Ltd

ever, FEL equations can not appropriately describe cases involving ultra-short pulse (i.e. broad bandwidth) seed lasers and off-resonant seed lasers. In this paper, a three-dimensional algorithm is developed for characterizing the laser-beam interaction in an undulator, which is built on the fundamental basis of electrodynamics, i.e. the electron's behavior is determined by the magnetic field and the laser electric field in time domain. With the help of the algorithm, several issues of great interest, such as the detuning effect in a laser-heater, the carrier envelope phase effect of a few-cycle laser in ultra-short X-ray FEL schemes and the output wavelength tuning in a high gain harmonic generation (HGHG) FEL, are numerically investigated.

## 2 Beam dynamics

Suppose a planar undulator with a sinusoidal magnetic field in the  $y$  direction and a period length  $\lambda_u$  in the  $z$  direction. Then consider a relativistic electron beam with an average energy of  $\gamma_0 mc^2$  and a coherent laser with wavelength  $\lambda_s$  entering the planar undulator together: one may observe the electron's transverse wiggling motion and the longitudinal "figure-eight" oscillation. Such a trajectory gives rise to energy exchange between the electron beam and the laser electric field. We denote the wave numbers of the seed laser and the undulator magnets by  $k_s = 2\pi/\lambda_s$  and  $k_u = 2\pi/\lambda_u$ , respectively. Then, the magnetic field distribution of the planar undulator can be written as

$$B_y = B_0 \sin k_u z, \quad (1)$$

where  $B_0$  is the undulator peak magnetic field. The electric field of a seed laser with Gaussian distribution and a *rms* size of  $\sigma_x$ ,  $\sigma_y$  and  $\sigma_z$  can be represented as

$$E_x^2 = E_0^2 \sin^2 [k_s(z' - z_0) + \varphi_0] e^{-\frac{x^2}{2\sigma_x^2} - \frac{y^2}{2\sigma_y^2} - \frac{(z' - z_0)^2}{2\sigma_z^2}}, \quad (2)$$

where  $z_0$  is the initial relative position of the laser from the electron beam and  $\varphi_0$  is the carrier envelope phase of the laser. The diffraction effects of the laser field can be approximated by

$$\begin{aligned} \sigma_x(z) &= \sqrt{\sigma_{xw}^2 + \frac{k_s^2(z - z_w)^2}{4\sigma_{xw}^2}}, \\ \sigma_y(z) &= \sqrt{\sigma_{yw}^2 + \frac{k_s^2(z - z_w)^2}{4\sigma_{yw}^2}}, \end{aligned} \quad (3)$$

where  $\sigma_{xw}$  and  $\sigma_{yw}$  denote the laser size at the longitudinal waist position  $z_w$ . Then the electron beam's

motion satisfies the law of electrodynamics,

$$\gamma m \frac{dv}{dt} = eE - ev \times B. \quad (4)$$

In the presence of the transverse wiggling motion of the electron beam and the transverse field of the seed laser, an energy exchange between the electrons and the electromagnetic field is expected as

$$mc^2 \frac{d\gamma}{dt} = eE_x \frac{dx}{dt}. \quad (5)$$

On the basis of Eqs. (1)–(5), a three-dimensional (3D), time-dependant code is built to numerically study the laser-beam interaction in an undulator. The initial electron beam distribution is loaded from GENESIS [23] to remove the effect of finite electron numbers and the integral step of each undulator period is set as 100 for an accurate solution. To check the validity of the algorithm, in the case of an infinitely long seed laser and an infinitely long electron beam, several comparative studies have been carried out by using steady-state mode of GENESIS and good agreement has been observed.

## 3 Detuning effect of a laser-heater

The bright electron beam required for a hard X-ray FEL suffers from microbunching instability in the magnetic bunch compressors, which may increase the slice energy spread beyond the FEL tolerance. Thus, a laser-heater [11–13] has been suggested to increase the slice energy spread of the electron beam by an order of magnitude to provide strong Landau damping against the microbunching instability without degrading the FEL performance. Such a system has been designed and demonstrated in LCLS [14] and is now incorporated in almost all short-wavelength FEL projects.

The LCLS laser-heater system modulates the energy of a 135 MeV electron bunch with a 758 nm IR laser in a short undulator, enclosed within a four-dipole chicane. The LCLS laser-heater undulator gap can be controlled remotely to change the undulator magnetic field and hence the resonant condition. Theoretically, the detuning effect of the laser-beam interaction in a laser-heater undulator is given by

$$\frac{\Delta E(\lambda_r)}{\Delta E(\lambda_s)} = \frac{\sin \left[ \pi N \frac{\lambda_r - \lambda_s}{\lambda_s} \right]}{\pi N \frac{\lambda_r - \lambda_s}{\lambda_s}}. \quad (6)$$

To understand the lasing effect when the undulator is out of resonance, we simulate the laser-beam interactions by scanning the undulator filed strength

from 0.18 to 0.68 T (i.e. the undulator resonant wavelength from 0.6 to 3.6 times of 758 nm IR laser). Variation in the electron beam laser-induced slice energy spread is illustrated in Fig. 1.

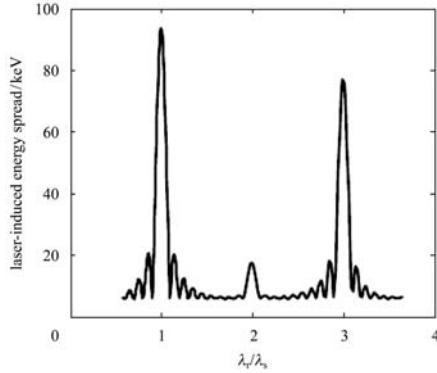


Fig. 1. Laser-induced *rms* slice energy spread vs. laser-heater undulator resonant wavelength obtained in simulation. The peak power of the IR laser is about 100 MW.

According to Fig. 1, the LCLS laser-heater presents a FWHM resonance width of 81 nm around 758 nm, the central wavelength of the IR laser, which is consistent with the result obtained from Eq. (6). A similar curve has been demonstrated in the LCLS laser-heater experiment [14] and the seeded FEL experiment at the Shanghai deep ultraviolet FEL [26]. Moreover, due to the relatively high coupling of the odd harmonic radiation and the electron beam in a planar undulator, when the laser-heater undulator is set to be resonant at 2274 nm, i.e. the 758 nm IR laser is the 3rd harmonic of the laser-heater undulator; effective energy modulation is also obtained.

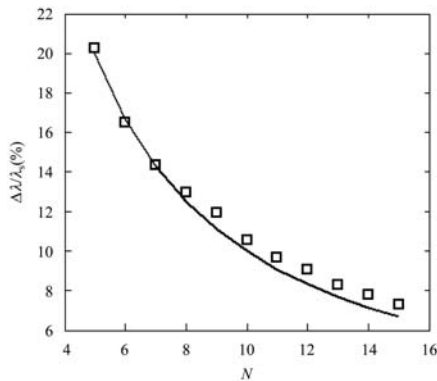


Fig. 2. The relative bandwidth of a laser-heater vs. laser-heater undulator period number  $N$ , the line is from the inverse scaling law and the squares are from simulation.

Low-gain FEL theory predicts an inverse scaling law of the bandwidth with the undulator periods number. Based on the LCLS laser-heater parameters, we also obtain the dependence of the relative

resonance bandwidth on the undulator period number using the proposed 3D code, as shown in Fig. 2, which agrees well with the prediction by the low-gain theory.

#### 4 Carrier envelope phase effects of few-cycle laser in ultra-short FEL pulse scheme

To generate attosecond pulses from an intense seed laser via an FEL mechanism, the electron beam density has to be modulated on an attosecond scale. The coherence of the density modulation, known as harmonic bunching, is crucial to the properties (coherence, power, pulse duration, etc.) of the generated attosecond pulses. Therefore, increasing effective electron beam density modulation is of great interest to the FEL community [8, 9]. Recently, a novel FEL scheme with remarkably high harmonic bunching, called echo-enabled harmonic generation (EEHG) [10, 27], was proposed, based on which, a series of proposals [28–30] are suggested for the generation of coherent attosecond X-ray pulses. In these ultra-short FEL pulse schemes, various high-intensity, few-cycle lasers are introduced to generate a large energy chirp in the electron beam phase space. However, the CEP effects of the few-cycle laser were not taken into account in the existing reports.

Here, we discuss the effects of the few-cycle seed pulse carrier-envelope phase (CEP) on output FEL performance. We take the EEHG-assisted attosecond X-ray pulse scheme as an example, and consider an 800 nm seed laser with an FWHM pulse duration of 2 fs, and assume that the beam parameters and the undulator are similar to those in Refs. [28, 30]. In reality, the electric field is nonperiodic in the 2 fs laser pulse and, as shown in Fig. 3, the density modulation on an attosecond scale is highly relevant to the CEP of the 2 fs seed laser pulse. It is found that since the optimized output wavelength is determined by the energy chirp induced by the 2 fs laser [30], CEP shift will inevitably be accompanied by an offset of the output FEL wavelength. However, the Fourier transform of the longitudinal beam distributions in Fig. 3 indicates that within the CEP shifts of  $0.5\pi$ , the FEL wavelength offset is almost neglectable compared with the intrinsic bandwidth of the output attosecond pulse.

Figure 3 also shows that the arrival time of the attosecond FEL pulse with respect to the few-cycle seed pulse is inversely proportional to the CEP shifts of the few-cycle laser, which was demonstrated in a

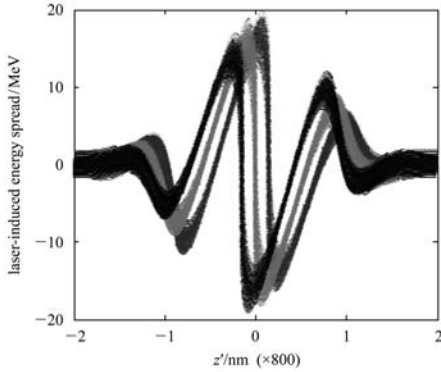


Fig. 3. Different longitudinal electron beam distribution before entering the radiator with respect to the different carrier envelope phase of 2 fs IR laser. Gray:  $\varphi_0=0.25\pi$ , White:  $\varphi_0=0.5\pi$ , Black:  $\varphi_0=0.75\pi$ .

further study, as illustrated in Fig. 4. Thus, in a pump-probe experiment, accurate time interval control can be realized by changing the CEP of the 800 nm few-cycle pulse. To our knowledge, the minimum CEP jitter under phase stabilization technology is the  $5^\circ$  [31] level, which corresponds to 37 attosecond resolution. Therefore, by locking shot-by-shot CEP [31], the time interval between the infrared pump pulse and the soft X-ray attosecond probe pulse can be stably controlled and shifted with a precision of about tens of attoseconds. Recently, various single-shot CEP measurement techniques without CEP stabilization were experimentally demonstrated [32, 33], in which, a precision as high as  $\pi/300$  can be guaranteed at an optimum measurement point. With the online CEP measurement using such technology, an accurate time interval with 4.4 attosecond resolution can be obtained between the 800 nm few-cycle seed laser and the generated ultra-short X-ray pulse, even without the above-mentioned CEP stabilization.

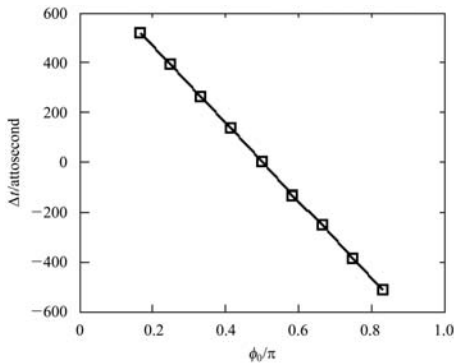


Fig. 4. The relative arrival time of the attosecond X-ray pulse vs. the CEP of the 2 fs, 800 nm laser.

## 5 Wavelength tuning of HGHG

Output wavelength tuning is one of the most

important features for FEL design. In a FEL starting from shot noise, output wavelength tuning can be easily realized by adjusting the FEL resonant condition. However, in a seeded FEL scheme, e.g. an HGHG, the seed laser usually has picosecond order pulse length and a narrow bandwidth comparable to the FEL pierce parameters [21]. Thus, the output wavelength of HGHG is absolutely determined by the seed laser. As is generally understood, altering the output wavelength of HGHG is a time- and effort-consuming procedure. Therefore, output wavelength tuning of HGHG is of great interest, and an HGHG FEL with tunable wavelength based on an accelerator technique has been demonstrated [34]. Recently, an HGHG FEL seeded by a few-cycle laser has been suggested for obtaining a tunable output wavelength [35–38]. In previous reports, the interaction between the electron beam and the few-cycle laser was investigated by the undulator-period-averaged equations [21–25] in time domain or one-dimensional multi-frequencies equations [36, 37] in spectral domain. In this section, using the proposed 3D algorithm in time domain, the beam dynamics in the modulator of an HGHG FEL is investigated.

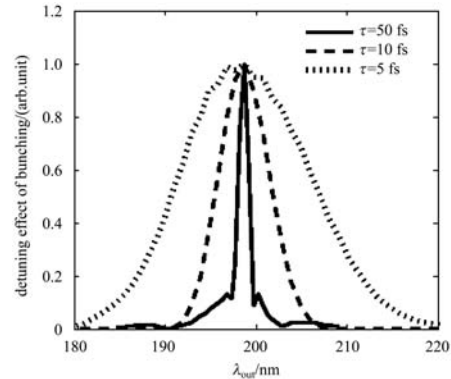


Fig. 5. The output bunching factor under different pulse durations of the 795 nm seed laser.

We set a group of parameters close to the 4th harmonic HGHG at NSLS SDL [39]. The seed laser is a Ti: sapphire laser with a central wavelength of 795 nm, which is synchronized with the electron beam. Three cases with *rms* seed laser durations of 50, 10 and 5 fs are studied, respectively. According to the simulation, the detuning effects of the bunching factor around the 4th harmonic are shown in Fig. 5. It is clear to see that some output wavelength tuning ability is recovered by using a short seed pulse. Furthermore, the simulated dependence of the output bunching tunability on the seed pulse duration is shown in Fig. 6. The tuning range is almost inversely proportional to the *rms* seed pulse duration, which is

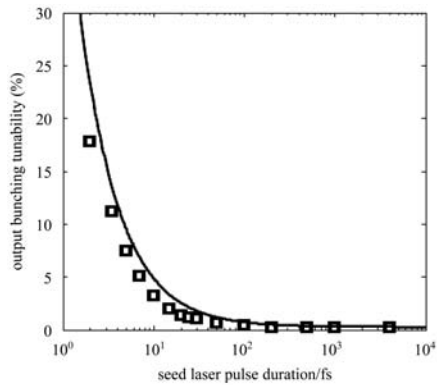


Fig. 6. The output bunching tunability around the 4th harmonic of seed laser .vs. the *rms* pulse duration of the 795 nm seed laser. The line is from theoretical estimate in Refs. [36, 37] and the squares are from the 3D simulation in time domain.

reasonably consistent with the theoretical estimates in Refs. [36, 37] and the 2% fluctuation of the output spectrum in the 4th harmonic HGHG experiment at NSLS SDL [39, 40].

## 6 Conclusions

In this paper, we report a three-dimensional, time-domain algorithm for beam dynamics, including the magnetic field of an undulator and the electric field of a coherent laser. Using the algorithm, we numerically discuss the detuning effect in a laser-heater undulator, the carrier-envelope phase effect of a few-cycle laser in ultra-short FEL pulses scheme and output wavelength tuning in an HGHG FEL. The simulated results are very consistent with theories and early works. It is worth stressing that the laser-beam interaction model in an undulator can be easily extended to an arbitrary magnetic field, such as dipole and quadrupole. It is helpful for some FEL frontier investigations, such as laser-induced energy modulation in a dipole field and its potential applications in FEL [41].

*The authors would like to thank T. Zhang, C. Feng, J. H. Chen, D. G. Li and B. Liu for helpful discussions.*

## References

- Murphy J, Pellegrini C, Bonifacio R. *Opt. Commun.*, 1985, **53**: 197
- SLAC Report No. SLAC-R-593, 2002
- DESY Report No. DESY-2006-097, 2006
- Ben-Zvi I et al. *Nucl. Instrum. Methods Phys. Res., Sect. A*, 1991, **304**: 181
- YU L H. *Phys. Rev. A*, 1991, **44**: 5178
- WU J H, YU L H. *Nucl. Instrum. Methods Phys. Res., Sect. A*, 2001, **475**: 104
- YU L H, DiMauro L, Doyuran A et al. *Phys. Rev. Lett.*, 2003, **91**: 074801
- Allaria E, Nino G D. *Phys. Rev. Lett.*, 2007, **99**: 014801
- JIA Q K. *Appl. Phys. Lett.*, 2008, **93**: 141102
- Stupakov G. *Phys. Rev. Lett.*, 2009, **102**: 074801
- HUANG Z, Borland M, Emma P et al. *Phys. Rev. ST Accel. Beams*, 2004 **7**: 074401
- Kim Y J et al. *Nucl. Instrum. Methods Phys. Res., Sect. A*, 2004, **528**: 427
- HUANG Z, Brachmann A, Decker F J et al. SLAC-PUB-13854, 2009
- Emma P et al. in *Proceedings of the 2009 IEEE Particle Accelerator Conference Vancouver*. BC, Canada, May, 2009
- Saldin E L, Schneidmiller E A, Yurkov M V. *Opt. Commun.*, 2002, **212**: 377
- Saldin E L, Schneidmiller E A, Yurkov M V. *Opt. Commun.*, 2004, **239**: 161
- Zholents A, Fawley W. *Phys. Rev. Lett.*, 2004, **92**: 224801
- Zholents A, Penn G. *Phys. Rev. ST Accel. Beams*, 2005, **8**: 050704
- Saldin E L, Schneidmiller E A, Yurkov M V, *Phys. Rev. ST Accel. Beams*, 2006, **9**: 050702
- Zholents A, Zolotarev M S, New J. *Phys.*, 2008, **10**: 025005
- Kroll N, Morton P, Rosenbluth M. *IEEE J. Quantum Elec-*
- tron, 1981, **QE-17**: 1436
- Bonifacio R, Narducci L M, Pellegrini C. *Opt. Commun.*, 1984, **50**: 373
- Pellegrini C. *Nucl. Instrum. Methods Phys. Res. A*, 1988, **272**: 364
- Reiche S. *Nucl. Instrum. Methods Phys. Res. A*, 1999, **429**: 243
- Fawley W. Lawrence Berkley National Laboratory internal note LBNL-49625, 2004
- ZHAO Z T, DAI Z M, ZHAO X F et al. *Nucl. Instrum. Methods Phys. Res. A*, 2004, **528**: 591
- XIANG D, Stupakov G. *Phys. Rev. ST Accel. Beams*, 2009, **12**: 030702
- XIANG D, HUANG Z, Stupakov G. *Phys. Rev. ST Accel. Beams*, 2009, **12**: 060701
- Zholents A, Penn G. *Nucl. Instrum. Methods Phys. Res. A*, 2010, **612**: 254
- YAN J, DENG H X, WANG D et al. *Nucl. Instrum. Methods Phys. Res. A*, 2010, **621**: 97
- Baltuska A et al. *Nature*, 2003, **421**: 611
- Wittmann T et al. *Nature Phys.*, 2009, **5**: 357
- Micheau S et al. *Phys. Rev. Lett.*, 2009, **102**: 073001
- Shaftan T, YU L H. *Phys. Rev. E*, 2005, **71**: 046501
- WU J H et al. *Opt. Express*, 2008, **16**: 3255
- DENG H X, WANG X T, DAI Z M. *Phys. Rev. ST Accel. Beams*, 2008, **11**: 040703
- DENG H X, DAI Z M. *J. Phys. D: Appl. Phys.*, 2008, **41**: 115503
- Allaria E et al. *EPL*, 2010, **89**: 64005
- WANG X J et al. *Proceedings of the 2006 Free Electron Laser Conference*. Berlin, Germany, 2006
- QIAN H, Hidaka Y, Murphy J B et al. BNL-82276-2009-CP, 2009
- DENG H X, YAN J, WANG D et al. *Nucl. Instrum. Methods Phys. Res. A*, 2010, **622**: 508